

## Acute and obtuse rhombohedrons in the local structures of relaxor ferroelectric $\text{Pb}(\text{Mg}_{1/3}\text{Nb}_{2/3})\text{O}_3$

Nanoscale heterogeneous structures play a crucial role in the appearance of gigantic susceptibilities and the associated novel phenomena in solids. Relaxor ferroelectrics have attracted much attention in the past few decades due to their complex local structures, puzzling mechanisms, and potential applications as high-performance electromechanical transducers based upon their excellent piezoelectric properties. However, because the nanoscopic heterogeneity inherent to relaxors creates challenges, the microscopic origin of the outstanding piezoelectric properties of relaxor-based ferroelectrics is uncertain.

X-ray fluorescence holography (XFH) is a model-free bulk sensitive technique to determine the local structure, enabling the 3D atomic environment around a selected element to be visualized within a radius of a few nanometers at an atomic resolution. These features make XFH method ideally suitable to investigate nanoscale heterogeneous structures in solids [1]. In this work, we investigate the local-three-dimensional (3D) atomic arrangements around the  $\text{Pb}^{2+}$  and  $\text{Nb}^{5+}$  ions in a prototypical relaxor [2], ferroelectric  $\text{Pb}(\text{Mg}_{1/3}\text{Nb}_{2/3})\text{O}_3$  (PMN) [3,4], using XFH.

The experiments were carried out at beamline **BL22XU**. XFH data were recorded at incident X-ray energies between 19.0 - 23.5 keV in 0.25 keV steps. **Figure 1(a)** shows the details of the experimental setup. Using a cylindrical graphite-crystal energy analyzer, Nb  $K\alpha$  (16.61 keV) and Pb  $L\alpha$  (10.55 keV) fluorescent X-rays from the sample were analyzed and focused onto an avalanche photodiode (APD), respectively. The measurement time for one energy hologram was about 3 h. **Figure 1(c)** shows a measured Nb hologram pattern taken at 20.0 keV. The hologram data were symmetrized using the average  $Pm\bar{3}m$  cubic symmetry of the sample (**Fig. 1(b)**) and the X-ray standing wave lines, and then extended to the  $4\pi$  sphere as shown in **Fig. 1(d)**. The 3D real-space atomic images around Nb and Pb were reconstructed from the multi-energy holograms using Barton's multiple energy algorithm [5].

**Figure 2(a)** shows the reconstructed atomic images on the (110) plane through the emitter Nb. Pb atomic images are clearly visible at the ideal positions, and obviously elongated along the radial direction. All of the Nb/Mg atoms on the B sites are hardly observed, indicating that the Nb/Mg atoms are largely disordered because the image intensity of an atom is reduced by its fluctuations. The Pb atoms are visible around the emitter Nb due to the atomic correlation between the Pb and Nb atoms. Only the nearest Pb atoms exhibit

$\langle 111 \rangle$  correlations with Nb. **Figure 2(b)** shows a fine 3D image of the first neighboring Pb atoms at the  $\frac{111}{222}$  positions. The cube indicates 1/8 of the unit cell of PMN. Surprisingly, four remarkable images are visible along the  $\langle 111 \rangle$  direction, which are labeled 1-4 **Fig. 2(b)**. The interatomic distances between the central Nb and these four Pb images are 2.73 Å, 3.21 Å, 3.71 Å, and 4.25 Å. The Pb1 and Pb4 images show a center symmetry with respect to the ideal position (3.5 Å).

Next, atomic images around the emitter Pb were reconstructed using the Pb  $L\alpha$  holograms to evaluate the Pb-Pb correlation. Since only the 200, 220, and 111 atomic images are visible in **Figs. 2(c)** and **2(d)**, a body center-like  $2a_0 \times 2a_0 \times 2a_0$  superlattice structure emerges ( $a_0 = 4.05$  Å). The Pb atoms around the emitter Nb are more visible (**Fig. 2(a)**), suggesting that the stability of the Pb atoms is relatively lower than the Nb atoms.

The rhombohedral distortion explains well the separation of the Pb images in **Fig. 2(b)**, and our calculations show that the rhombohedral deformation of the perovskite cube with rhombohedral angles of  $77.0^\circ$  and  $100.6^\circ$  give rise to two Pb-Nb interatomic distance pairs of 3.23 and 4.22 Å, and 2.78 and 3.71 Å, respectively. These values are close to the experimentally observed ones, confirming that there are acute and obtuse rhombohedrons in the local

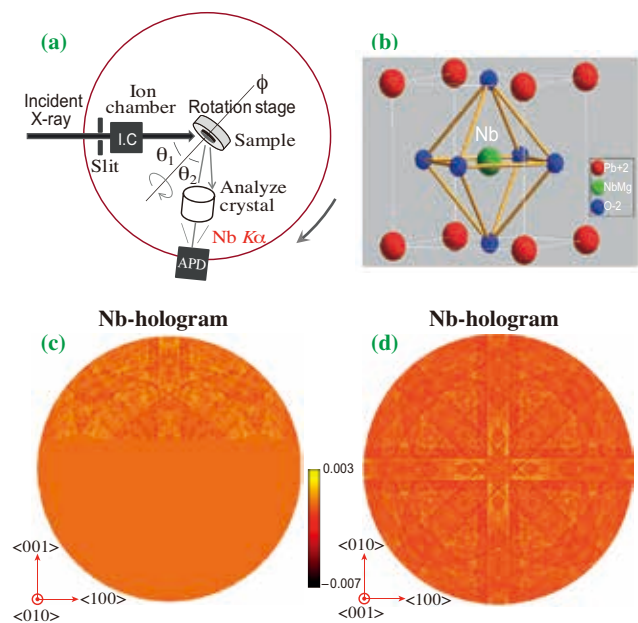


**Fig. 1.** (a) XFH experimental setup. (b) Ideal structure of perovskite PMN. (c) Nb hologram of PMN on a spherical surface. Lower areas indicate the part of the full holographic information that could not be measured. (d) Extended  $4\pi$  hologram of Nb hologram in (c).

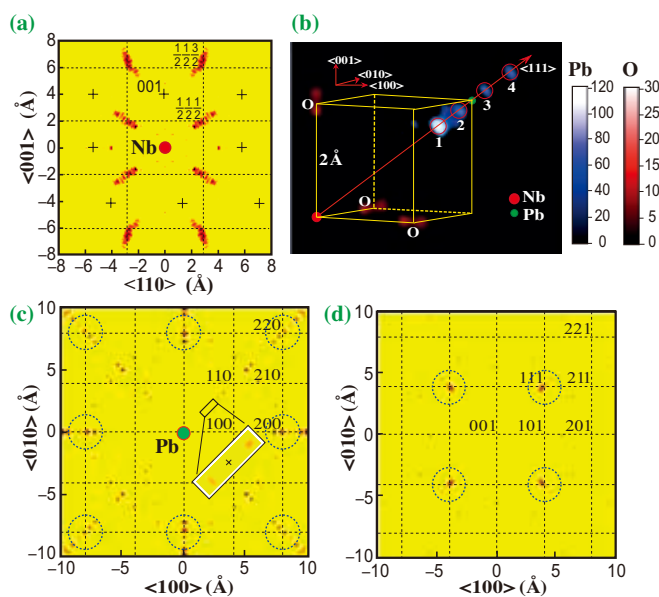


Fig. 2. Atomic images in PMN. (a) (110) plane around the emitter Nb. Intersections of dotted lines indicate the ideal atomic positions of Pb atoms in (a), (c), and (d). Crosses in (a) indicate the ideal positions of Nb/Mg. (b) 3D images of the nearest Pb atoms around Nb. Atomic images around the emitter Pb on the (001) plane at (c)  $z = 0 \text{ \AA}$  and (d)  $z = 4 \text{ \AA}$ .

structure of PMN (Fig. 3(a)).

To understand the Pb2 and Pb3 images in Fig. 2(b), we introduced a disk-like 2D Gaussian distribution with a mean-square displacement ( $\sigma_a$ ) and calculated the image intensities of the Pb2 and Pb3 atoms by changing the value of  $\sigma_a$ . The calculated atomic images with  $\sigma_a = 0.19 \text{ \AA}$  agree well with the experimental data, which indicates that there are two distorted rhombohedrons in PMN for the Pb-Nb correlations and a nanoscale antidistortive transformation. Combining these two rhombohedral unit cells (Fig. 3(c)), constructs a body-center-like 3D network structure, which is comprised of positionally

stable Pb ions and off-centered Pb and Nb ions fluctuating around their corresponding ideal perovskite position. The estimated size of the corresponding domain is 1-2 nm suggesting that the fluctuating Pb and Nb ions are responsible for the characteristic broad relaxation spectrum observed in PMN.

The present work demonstrated the new potential of XFH to characterize disordered systems and to provide more detailed structural information. This capability is a powerful tool in understanding the relations between the properties and the local structures in disordered functional materials.

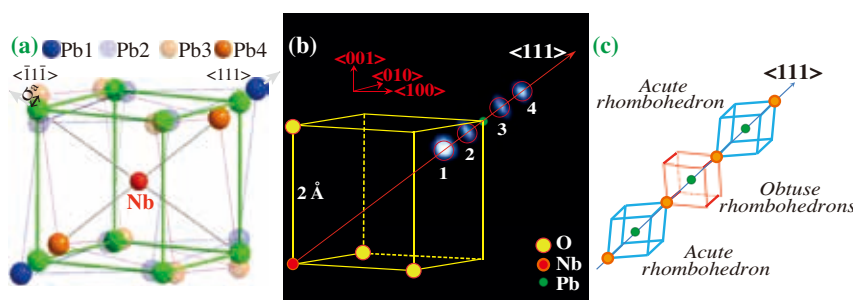


Fig. 3. Reproduction of the nearest Pb images around Nb, based on a rhombohedral transformation model of the unit cells. (a) Schematic of transformation of the unit cell from cubic to acute and obtuse rhombohedrons.  $\sigma_a$  is the FWHM of the 2D Gaussian distribution of Pb2 and Pb3 parallel to the (111) plane. (b) 3D images of the nearest Pb atom around Nb reconstructed from the calculated holograms with  $\sigma_a = 0.19 \text{ \AA}$ . (c) 3D network of acute and obtuse rhombohedrons.

Wen Hu<sup>a,\*</sup>, Kouichi Hayashi<sup>b</sup> and Kenji Ohwada<sup>c</sup>

<sup>a</sup> National Synchrotron Light Source II, Brookhaven National Laboratory, USA

<sup>b</sup> Institute of Materials Research, Tohoku University

<sup>c</sup> SPring-8/JAEA

\*E-mail: wenhu@bnl.gov

## References

- [1] K. Hayashi *et al.*: J. Phys.: Condens. Matter **24** (2012) 093201.
- [2] W. Hu, K. Hayashi, K. Ohwada, J. Chen, N. Happo, S. Hosokawa, M. Takahashi, A.A. Bokov and Z.-G. Ye: Phys. Rev. B **80** (2014) 140103(R).
- [3] G.A. Smolenskii and A.I. Agranovskaya: Sov. Phys. Tech. Phys. **2** (1961) 2584.
- [4] A.A. Bokov and Z.G. Ye: J. Mater. Sci. **41** (2006) 31.
- [5] J.J. Barton: Phys. Rev. Lett. **67** (1991) 3106.